Pisa, 4 December 2009:

GG: GUIDELINES IN VIEW OF USING A LASER GAUGE

CONTENTS

- *Premise*
- *The signal*
- *The satellite and the experimental apparatus*
- *Accommodation of the laser gauge*

- *Premise*

It has been suggested by Slava Turyshev that the relative displacements of the GG test cylinders may be measured with a laser gauge derived from the type developed for SIM. It would replace the capacitance transducer currently designed for GG, and in use with the GGG prototype. A transducer based on laser interferometry would be sensitive only to differential displacements of the tests cylinders –such as an EP violation signal– and be in principle unaffected by any displacement in common mode. Note that the GG (and GGG) capacitance transducer –in its current version– requires the capacitance plates to be accurately centered in between the test cylinders for the common mode displacements not to give rise to spurious differential signals.

- *The EP violation signal*

The GG target to test the Equivalence Principle to 10^{-17} requires to detect relative displacements of the test cylinders of 0.5 pm at the orbital frequency (about $1.75 \cdot 10^{-4}$Hz). Because of the 1Hz co-rotation of the test cylinders together with the GG satellite, this signal will be detected by the read-out at the spin frequency. The relevant electronic noise that must be reduced below the signal is therefore the electronic noise at 1Hz. In the case of the capacitance transducer the required noise is 10^{-7} pF/√Hz at 1Hz.

The EP violation signal in the GG experiment is described in Figs.1&2. The signal recovery strategy is described in Fig. 3.

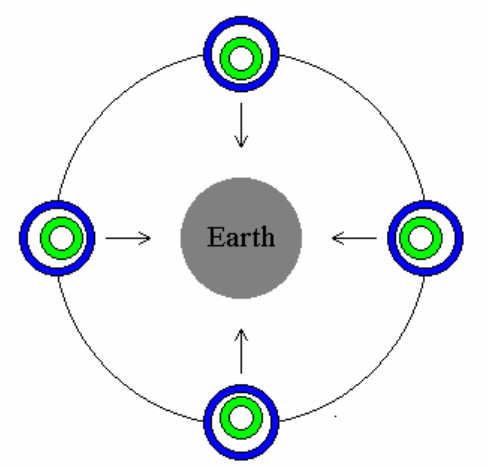

Figure 1: The EP violation signal in GG. Section in the plane perpendicular to the spin/symmetry axis of the GG outer and inner test cylinders (of different composition and weakly coupled in the plane) as they orbit around the Earth

inside a co-rotating, passively stabilized spacecraft (not shown). The centers of mass of the test cylinders are shown to be displaced towards the center of the Earth as in the case of a violation of the equivalence principle in the field of the Earth (indicated by the arrows). The signal is therefore at the orbital frequency ($1.75 \cdot 10^{-4}$ Hz). Figure 2 below shows how this signal is modulated by rotation around the symmetry axis. (The figure is not to scale).

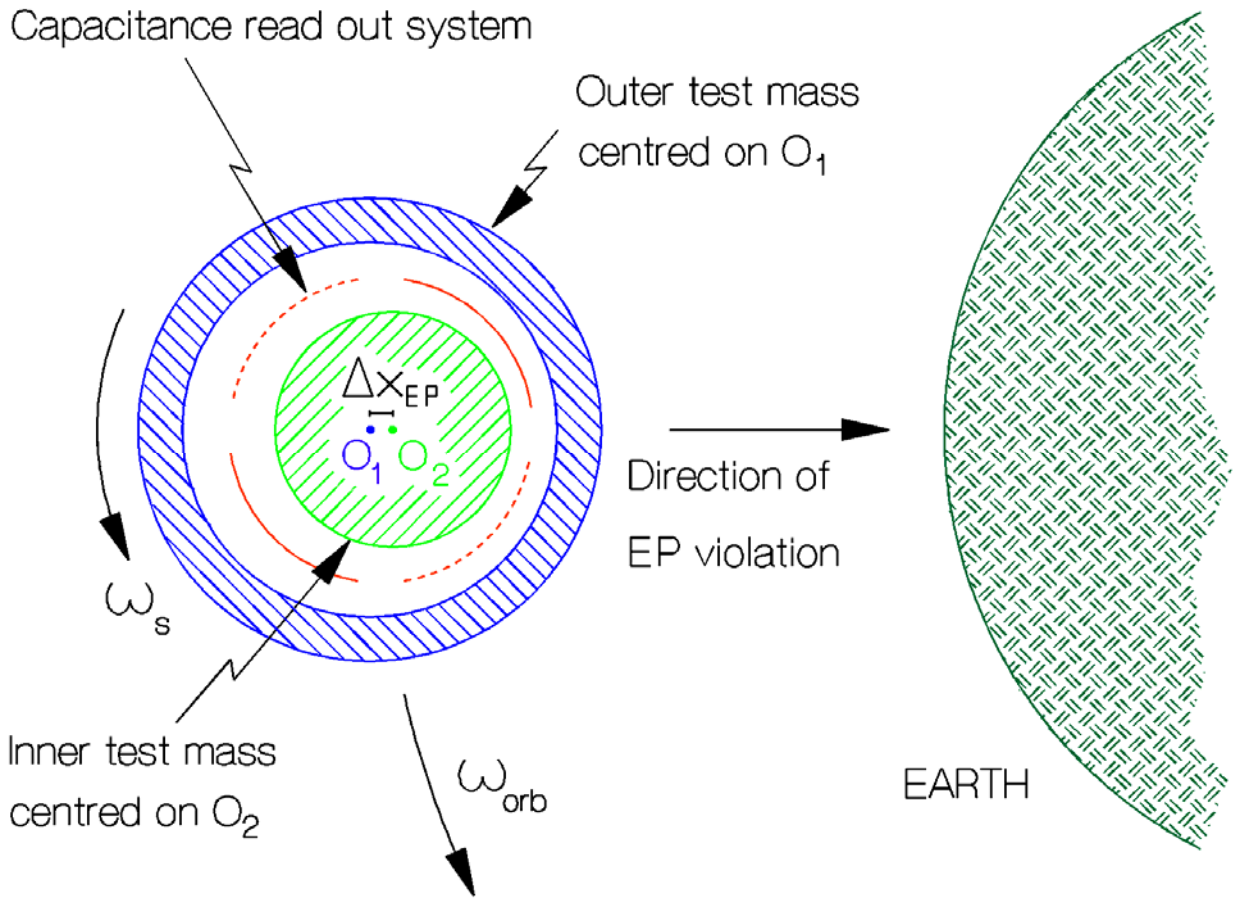

Figure 2: Modulation of the violation signal at the spin frequency. Section of the GG coaxial test cylinders and capacitance sensors in the plane perpendicular to the spin axis (not to scale). The capacitance plates of the read-out are shown in between the test bodies, in the case in which the centers of mass of the test bodies are displaced from one another by a vector $\Delta\vec{x}_{EP}$ due to an Equivalence Principle violation in the gravitational field of the Earth (e.g., the inner test body is attracted by the Earth more than the outer one because of its different composition). Under the (differential) effect of this new force the test masses, which are weakly coupled by mechanical suspensions, reach equilibrium at a displaced position where the new force is balanced by the weak restoring force of the suspension (the weaker the coupling, the larger the displacement), while the bodies rotate independently around O_1 and O_2 respectively. The vector of this relative displacement has constant amplitude (for zero orbital eccentricity) and points to the center of the Earth (the source mass of the gravitational field); it is therefore modulated by the capacitors at their spinning frequency with respect to the center of the Earth (1Hz in the current GG baseline). Note that in this design high frequency modulation of the signal is obtained without forcing the signal at the rotation frequency; this fact allows the rotation frequency to be higher than the coupling frequency (in fact much higher) without the signal being attenuated.

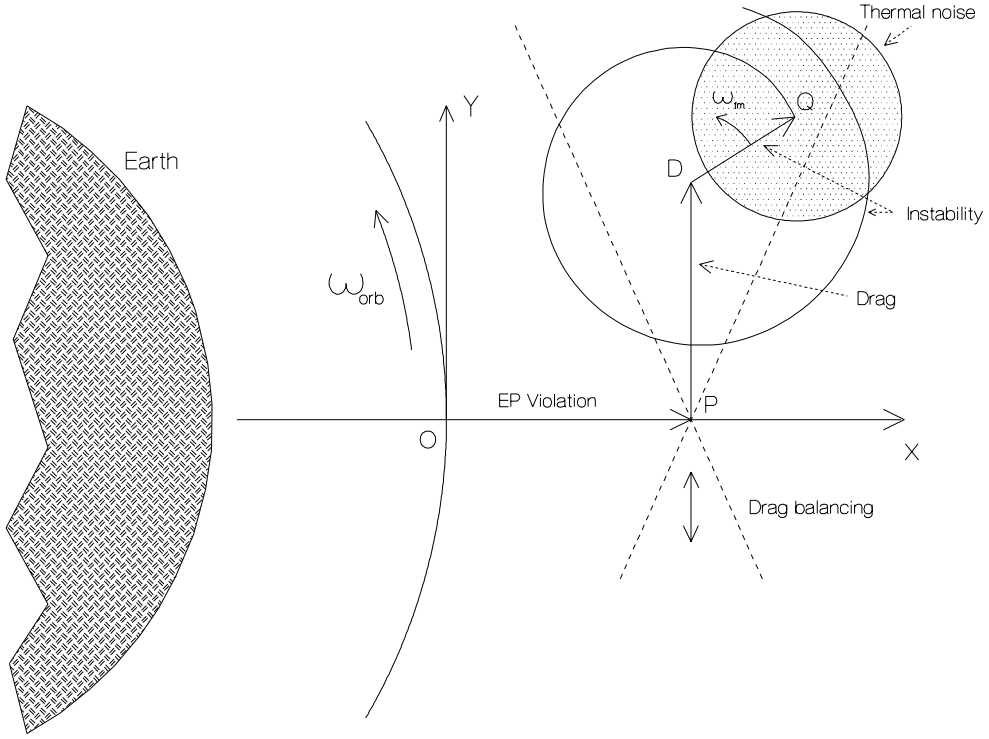

Figure 3: Qualitative representation, in the orbital plane, of the differential displacements obtained from the synchronous demodulation of the 2-phase 1 Hz signal. The *X* axis is fixed in the Earth-to-satellite direction; in this non spinning frame the ***OP*** vector represents the expected signal, namely a differential displacement, directed along the *X* axis and constant in amplitude (for zero orbital eccentricity, otherwise changing from perigee to apogee in a well knwon manner), of the two masses due to a violation of the Equivalence Principle. The perturbation ***PD*** due to an unbalanced atmospheric drag will be found in the area between the two dotted lines crossing in *P*: The angle between them is roughly 0.8 rad (which would slightly change with the satellite orbiting altitude), due to the fact that the drag has a variable component in the radial direction because of solar radiation pressure. Smaller contributions to the ***PD*** vector come from the Earth albedo, the Earth infrared radiation and, by a smaller amount, from the eccentricity of the orbit. By finely adjusting the lengths of the suspension arms (see Figure 10) the point *D* is displaced up or down inside this area, and brought close to *P*. In doing so, also the radial component of the drag is automatically balanced. The low frequency variations of the drag (not shown) will oscillate inside the same area. The vector ***DQ*** shows here the whirl instability before it is damped by the whirl control whose period in this (non spinning) frame is the natural frequency of oscillation. The circle around point Q represents the error in the measurement due to thermal noise of the mechanical oscillations built up during the integration time.

- *The satellite and its experimental apparatus*

The GG spacecraft (Figs. 4&5) has cylindrical symmetry and is passively stabilized by rotation around the symmetry axis (the axis of maximum moment of inertia) at 1Hz. The spacecraft body (Figs. 5&6), encloses –in a nested configuration– the PGB (Pico Gravity Box) and the GG differential accelerometer, all with cylindrical symmetry (Figs. 7&8).

The GG differential accelerometer is sensitive in the plane perpendicular to the spin/symmetry axis, which is close to the orbit normal.

The PGB is weakly suspended from the spacecraft body and the GG accelerometer is weakly suspended from the PGB. These are the only non-rigid "nodes" of the entire system (Fig. 9 & Table I). The whole system co-rotates at 1Hz, so that no motor is needed and no rotation and bearings noise is introduced. Co-rotation between the s/c outer skin and the PGB is tested and ensured (passively and also actively if needed). The PGB provides a vibration attenuation stage and serves as test mass for the Drag Free Control

loop; its relative displacements w.r.t. the spacecraft are sensed by capacitance bridges both in the (x,y) plane –perpendicular to the spin/symmetry axis z– and along z. In addition, the PGB is properly equipped to provide passive thermal stability of the GG accelerometer and allows some additional equipment to be located close to the accelerometer should it be needed or regarded as preferable.

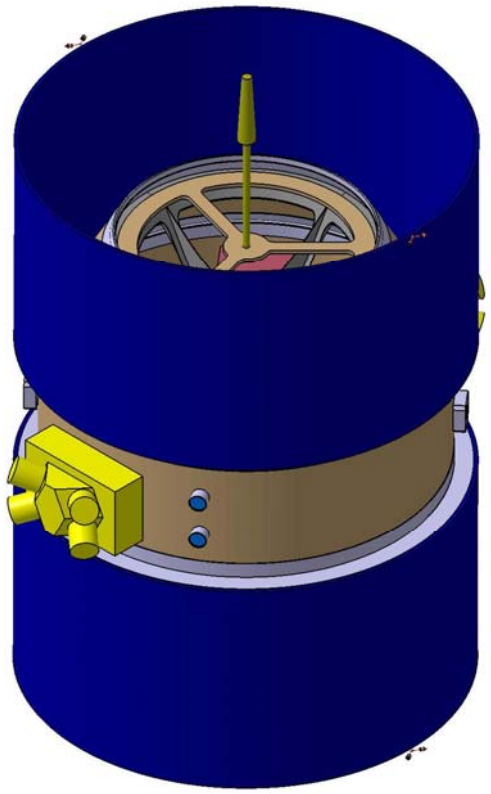

Figure 4: The GG cylindrical s/c (1.45 m central diameter) showing the solar panels (blue), the main body (light brown, see Fig. 5) with one antenna along the symmetry axis and the FEEP propulsion system (yellow).

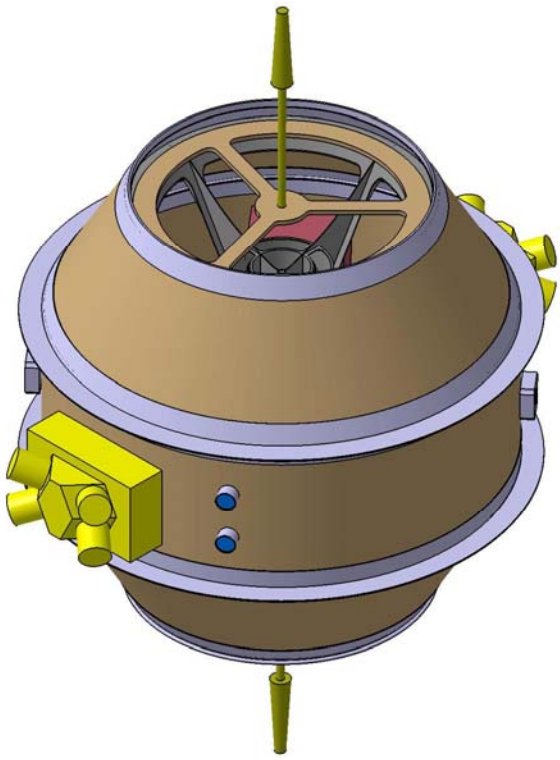

Figure 5: The spacecraft body carrying the GG experimental set-up (1.45 m central diameter).

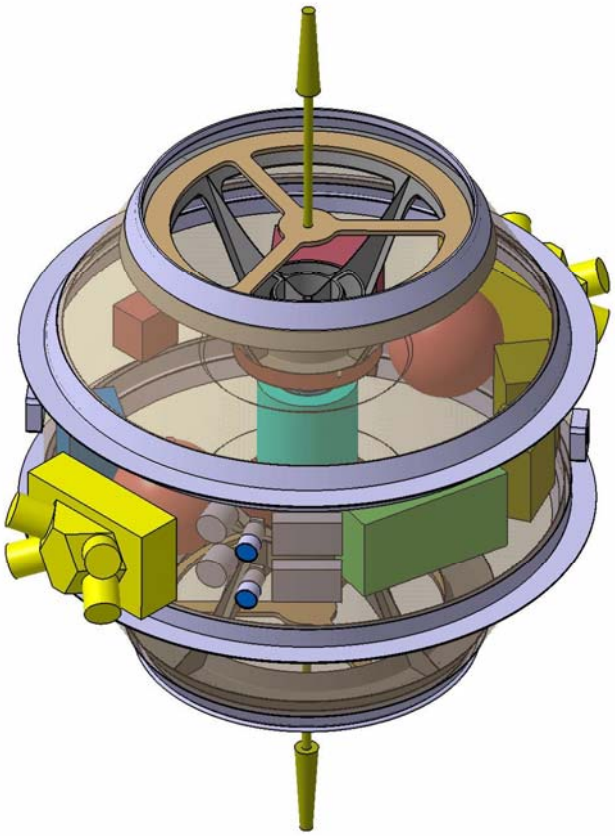

Figure 6: Transparent view of the spacecraft body. At its center is visible –here in light blue– the outer test cylinder of the GG accelerometer (better visible in Figs. 7&8)

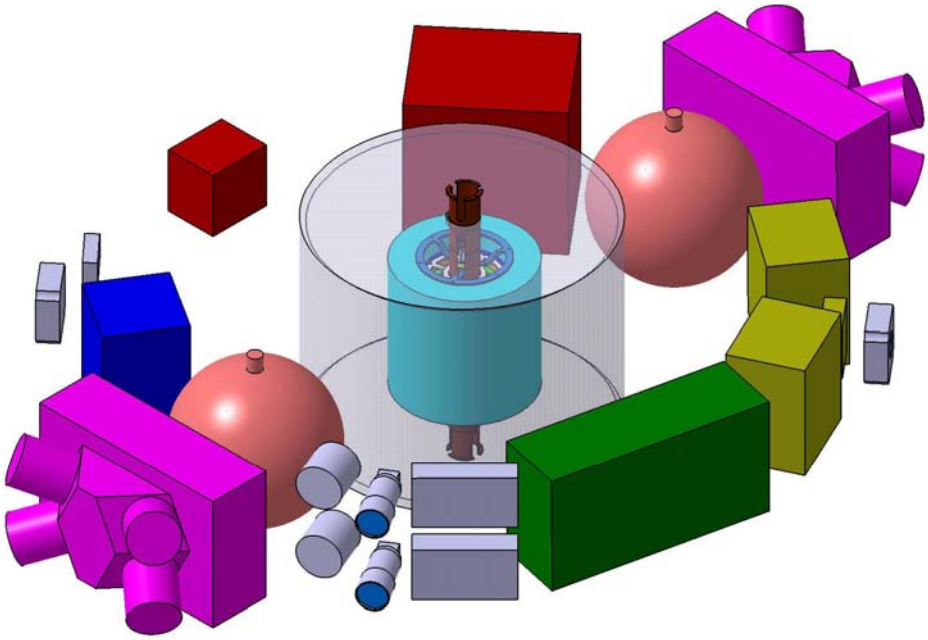

Figure 7: View inside the spacecraft body. The transparent cylinder is a schematic representation of the PGB, with its central shaft (in dark brown) at whose center the GG accelerometer is suspended as shown in Fig. 6 (the outer test cylinder of the accelerometer is shown here in light blue). The PGB is weakly suspended from the spacecraft body (suspensions not shown here).

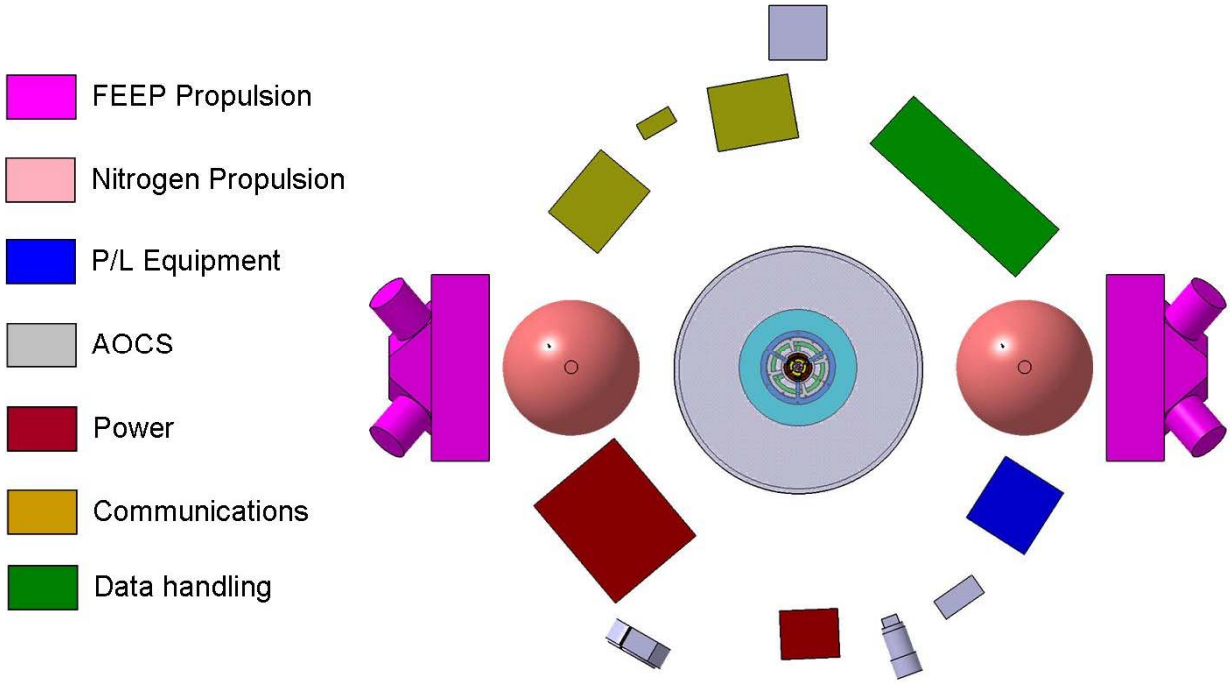

Figure 8: Top view of the apparatus shown in Fig. 7. At the center is visible the PGB shaft, with the GG accelerometer around it, enclosed by the PGB cylindrical body. All the rest is mounted on the spacecraft body.

The logical scheme of the GG dynamical system is shown in Fig. 9. The corresponding natural frequencies (periods) of oscillations are shown in Table I. Note that the lowest natural frequency is the frequency of natural oscillation of the test cylinders of the GG accelerometer relative to each other (differential mode). This ensures high sensitivity to differential effects, such as that of a possible EP violation. Such a low frequency (i.e. weak coupling) is made possible by absence of weight in space. As shown in the Table, all natural frequencies of oscillation are much smaller than the 1Hz rotation frequency. This ensures that all bodies are rotors in supercritical rotation. In such a condition the center of mass of a rotor self-centers close to its rotation axis, a physical condition very close to that of an ideal free rotor whose center of mass is lies on the rotation axis.

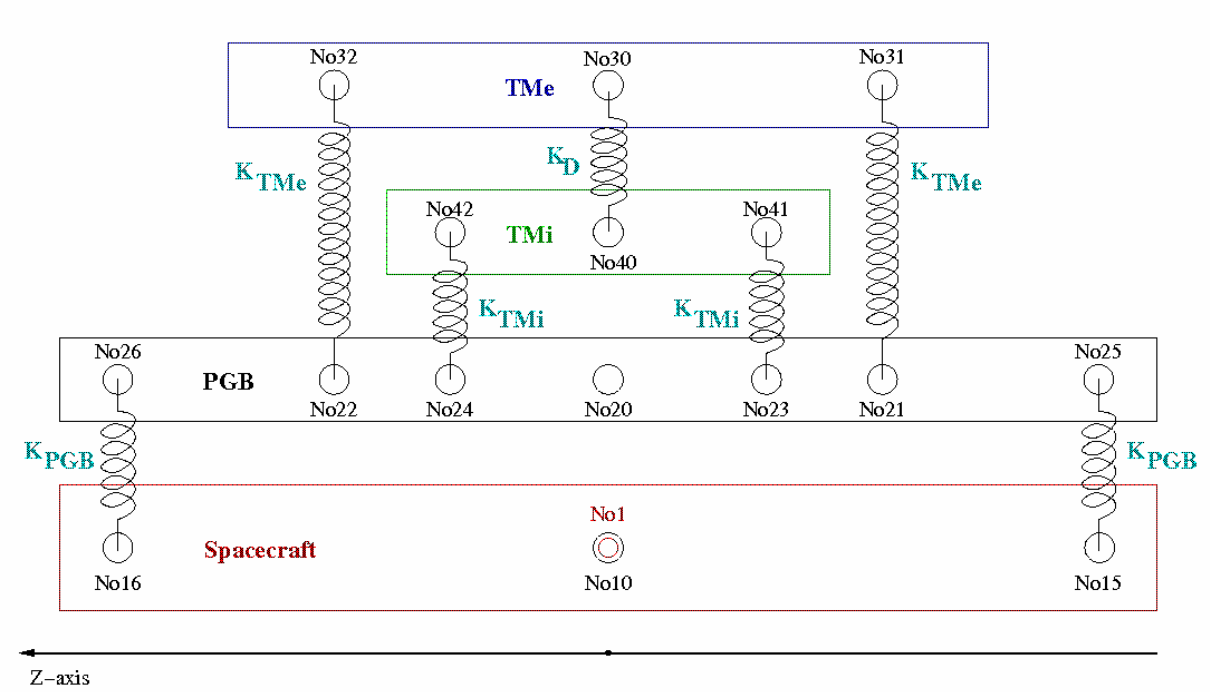

Figure 9: Logical scheme of the GG dynamical model implemented within DCAP software code for finite element simulation of the space experiment. The z axis is the spin/symmetry axis of the system; all elastic connections along z are very stiff; the plane of sensitivity is perpendicular to z. The GG simulator encompasses all bodies (spacecraft, PGB and 2 test masses), each one with its 6 degrees of freedom in 3D (3 for translation and 3 for rotation), mass and moments of inertia. All non rigid components of the system (sketched as springs) are implemented in the simulator with their designed stiffness (in the sensitive plane as well as in the z direction) and mechanical quality factors Q.

TABLE I: PERIODS (FREQUENCIES) OF THE NATURAL PERIODS OF OSCILLATIONS OF THE GG BODIES

	PGB-spacecraft		**GG accelerometer test masses**			
			Differential mode		*Common mode*	
	Period (s)	*Frequency (Hz)*	*Period (s)*	*Frequency (Hz)*	*Period (s)*	*Frequency (Hz)*
x,y *plane of sensitivity*	360	$2.8 \cdot 10^{-3}$	540	1.85·10-3	30	$3.3 \cdot 10^{-2}$
z *spin/symmetry axis*	30	$3.3 \cdot 10^{-2}$	*(no coupling of the test masses along z)*		30	$3.3 \cdot 10^{-2}$

The GG accelerometer scheme is shown in Figure 10 in a 2-D Section along the symmetry axis, and the caption helps to understand its design. A better understanding of the instrument can be obtained from Fig, 11 where several 3D charts derived from the construction drawings of the accelerometer show its structure, and how the cylindrical symmetry is respected. Then, Fig. 12 shows the "core" of the instrument, and how the test cylinders are coupled.

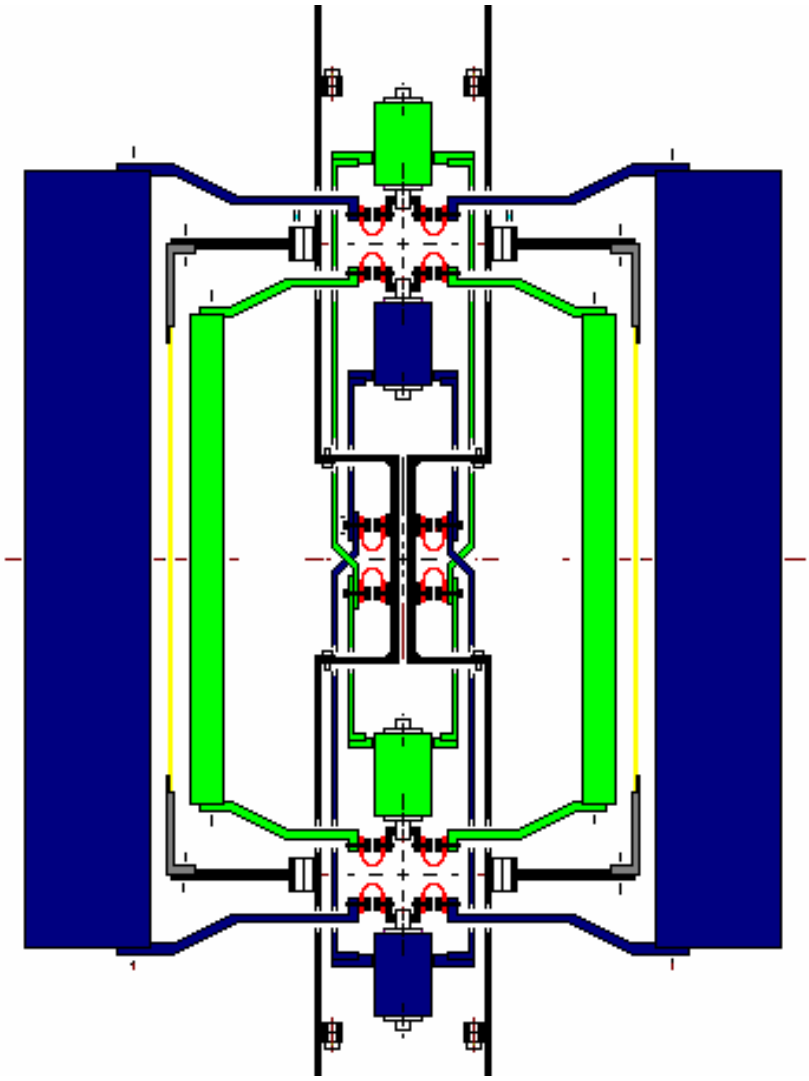

Figure 10: Baseline design of the GG accelerometer made of two test cylinders of different composition, shown in blue and green (section through the spin/symmetry axis). The figure is to scale; the external diameter of the blue test cylinder is 23 cm. The co-axial. co-centered test cylinders (weighing 10 kg each) are coupled to form a beam balance by being suspended at their top and bottom from the 2 ends of a coupling arm (suspensions are shown in red and described below). The coupling arm is made of 2 concentric tubes; each tube suspends one test cylinder at each end, which makes it asymmetric top/down –however, the two of them together form a symmetric coupling. Both tubes are suspended at their midpoints from the PGB central shaft (the longest vertical tube in the figure). Taken together, the system is "a balance" sensitive to differential forces acting between the cylinders in the plane perpendicular to the symmetry axis (plane of sensitivity), which makes it suitable for detecting an Equivalence Principle violation signal. The better the coupling arms are balanced, the better the system rejects effects acting in common mode on both test cylinders, the more sensitive it is to differential effects such as the target signal. The lengths of the coupling arms are adjusted for balancing and for centering along the axis by means of 4 inchworms, drawn in figure as small cylinders along the symmetry axis (2 in green, 2 in blue). The suspensions are in all cases $\cup$-shape (or $\cap$-shape) thin strips (shown in red), to be carved out of a solid piece of CuBe. At each connection there are 3 of them, at 120° from one

another (the planar section in figure shows 2 for explanatory purposes only). Finally, there are 4 capacitance plates in between the test cylinders (rigidly connected to the PGB suspension shaft; shown as 2 yellow lines in the planar section –see Fig. 11) to read-out the differential displacements in between the test cylinders in the sensitive plane.

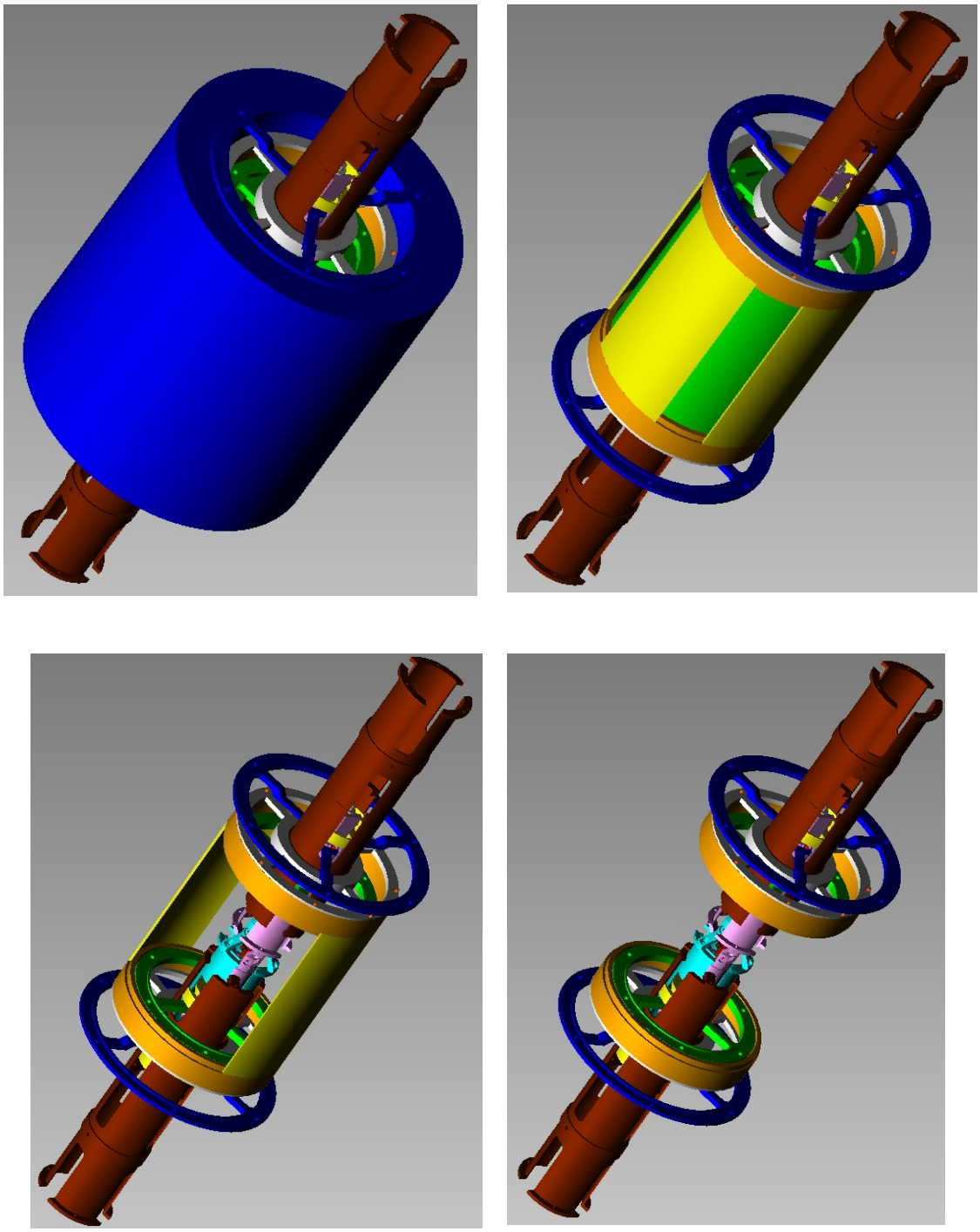

Figure 11: Details from the engineering drawings of the GG differential accelerometer showing the instrument parts from the "outside" (top figure) to the "inside". The brown central tube is the PGB shaft, with the coupling arms (in pink and pale blue inside it). The blue and green cylinders are the test masses, the yellow plates are the capacitance bridge plates designed to measure the relative displacements of the test cylinders.

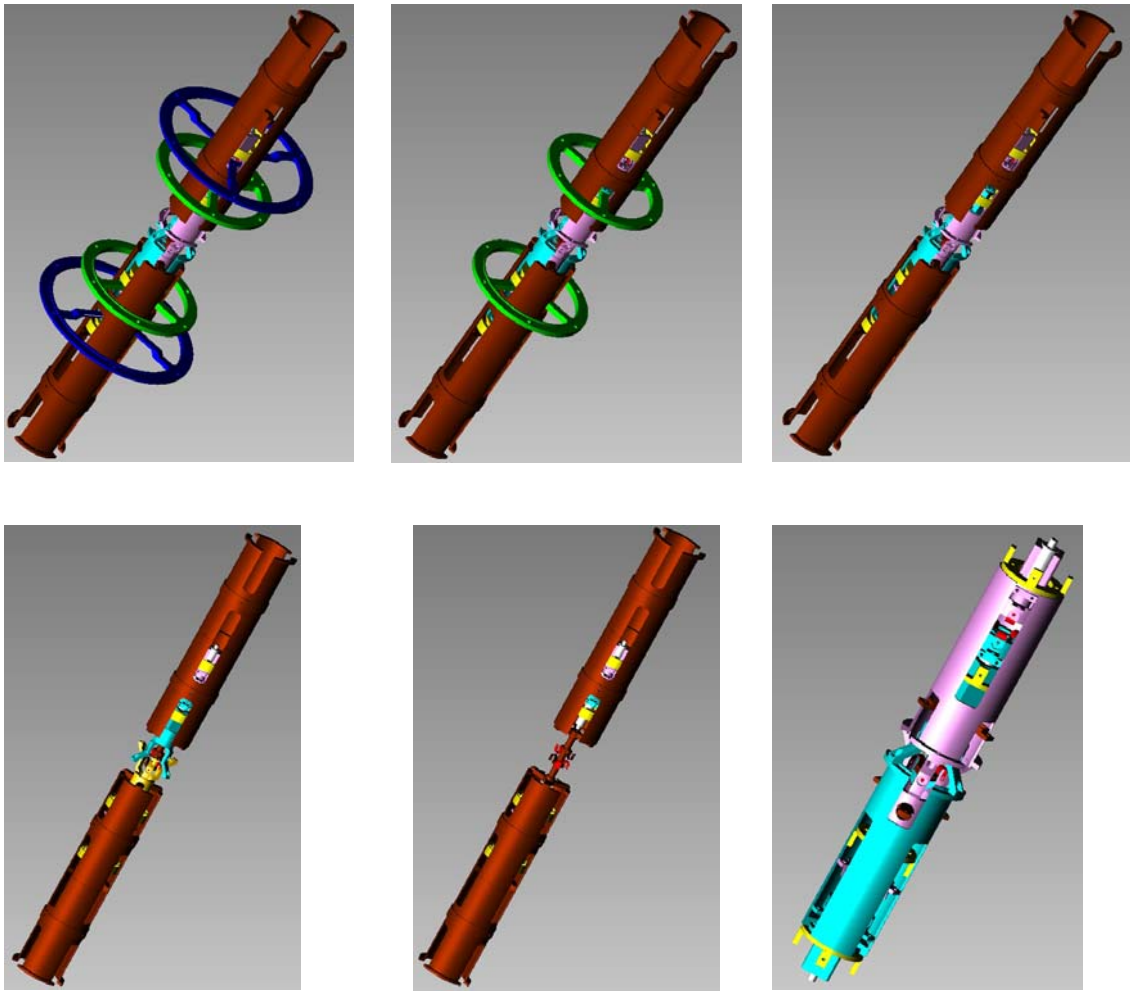

Figure 12: From previous figure: further details after removing components one by one. In the last picture only the coupling arm remains, and it is clear how it is made symmetric by putting together the two parts (pink and light blue). In the figure before the last, the PGB shaft is well visible, showing its center where the two pieces of the coupling arm are connected, each one with 3 U shaped laminar suspensions at 120° from each other.

- *Accommodation of the laser gauge*

Let us now remove the capacitance read-out and consider installing a laser interferometric gauge. Note that the capacitance bridges measuring the displacements of the test cylinders in the orthogonal directions of the plane perpendicular to the symmetry axis are rigidly connected to the PGB shaft; to remove them, in Fig. 11 we shall remove the 4 (yellow) capacitance plates, the 2 (brown) insulating rings, each one with the rings and spikes that connect it to the PGB (see Fig. 13). Note that, though not shown in the Figures, the electronics of the capacitance read-out would be located on a ring plate around the "free" PGB shaft above or below the test cylinders (as in GGG in the lab) with connection wires to the 4 capacitance plates (also via the PGB shaft) whose parasitic capacitances are properly taken into account in the circuit design. The PGB is powered from the spacecraft body via a contactless power coupler.

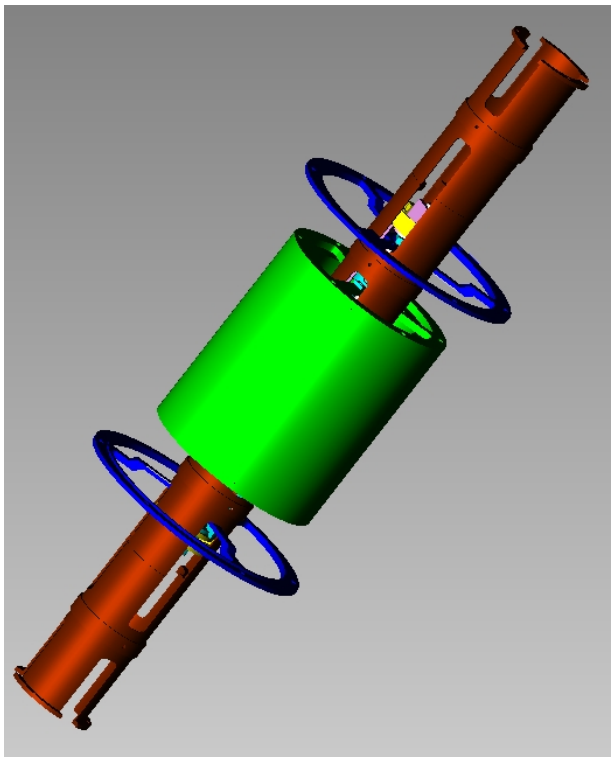

Figure 13: The GG accelerometer (the outer –blue– test cylinder is not visible to show the inner one) having removed completely the capacitance plates and their supports.

The laser gauge hardware and electronics should preferably be located on the cylindrical body of the PGB. Laser light from the PGB cylindrical body can be brought to a mirror on the outer surface of the inner test cylinder through a partially reflective mirror placed in a hole made on the outer test cylinder. Light reflected (after multiple reflections) by the inner and outer test cylinders can be collected by a detector located on the PGB cylindrical body and the digitized signal can be sent out to the spacecraft via an optical link. On the spacecraft the reference signal is also available, provided by an ad-hoc angular attitude and spin rate sensor; it allows coordinate transformation of the relative displacements of the test cylinder to the non rotating frame (see Fig. 14) where the signal of interest is expected at the orbital frequency.

By performing 2 such measurements (90° apart in azimuth) it is possible to obtain information on the relative displacements of the test cylinders in both directions of the sensitive plane; one could also have 4 (at 90° separation in azimuth).

The signal provides the interference fringes which contain the information on the time evolution of the relative displacements of the test cylinders. It will appear as a time series and its FFT component at the spin frequency and close to it will contain the signal of interest as well as various perturbing signals at close-by frequencies. After transformation to the LVLH non rotating system (Fig. 14) the lines can be separated out and represented as in Fig. 15.

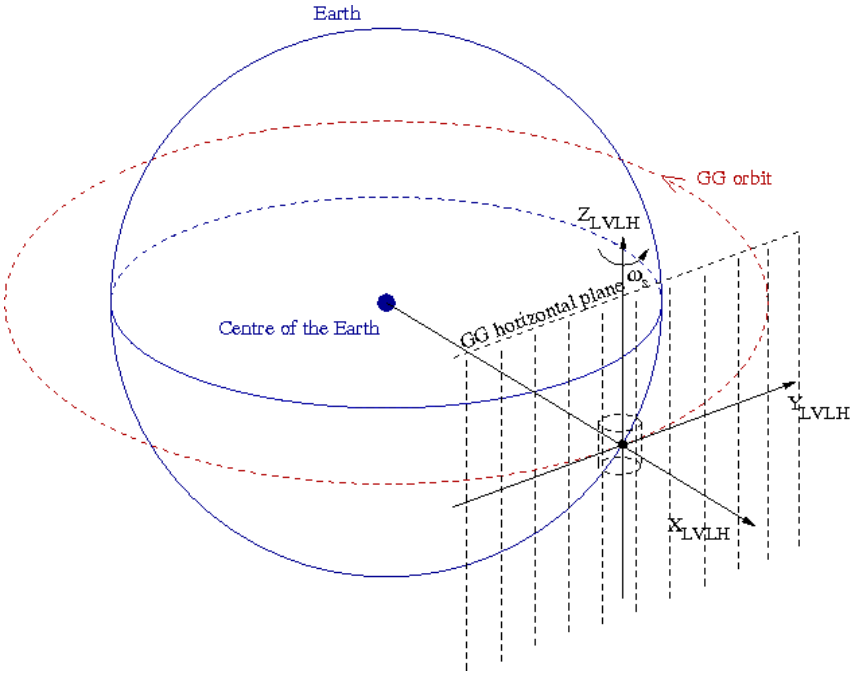

Figure 14: The Local Vertical Local Horizontal (non rotating) reference system

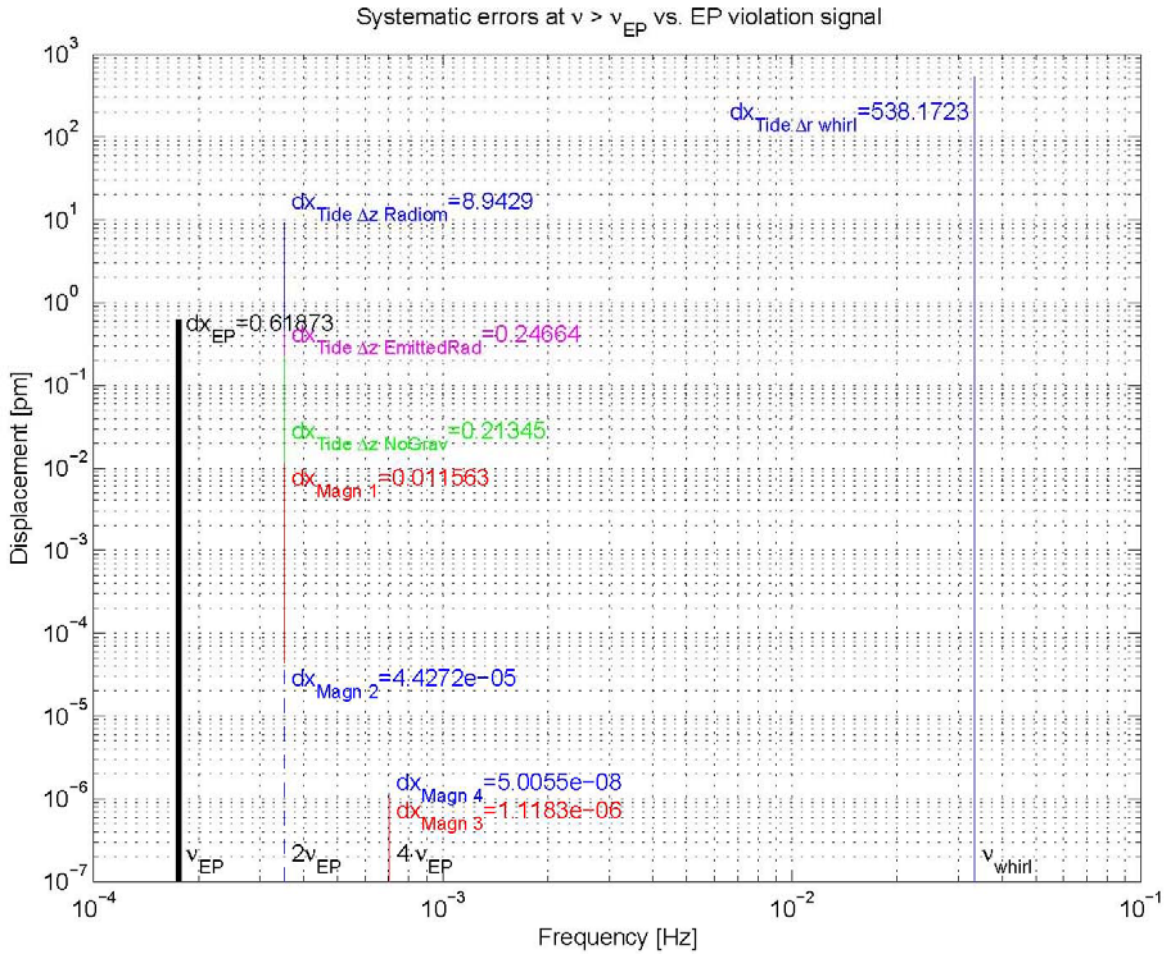

Figure 15: Graphical representation of the GG error budget as obtained from the Space Experiment Simulator. The mission requirements are embedded in the Simulator during a science run; the time series of the relative displacements of the test cylinders (which should be zero if Universality of Free Fall and the Weak Equivalence Principle hold!)

allows us to establish systematic and random errors. The plot reports major systematic errors only, caused by various (classical) perturbations, as function of their frequency (in the inertial frame) to be compared with the signal expected for an EP violation to 10^{-17} (indicated by the thick line, first from left). The relative displacement caused on the test masses by the signal and the various perturbations is expressed in picometers. The frequency of the signal is the satellite orbit frequency, indicated as ν_{EP}. It is apparent that even though in some cases the perturbing effects are larger than the signal, they are always sufficiently separated in frequency to be distinguished from it.

It would be important at this point: i) to describe the baseline design, the requirements and the constraints of the laser gauge for it to work and perform the task; ii) to estimate the mass, power and volume required by the laser gauge hardware and electronics iii) to establish the achievable sensitivity (NOTE: with the differential coupling of test cylinders reported in Table I, the GG target requires to detect 0.5 pm displacements at the (low) orbital frequency, while the relevant electronic noise is at the (high) 1Hz rotation/modulation frequency. With the capacitance transducer, the required noise is 10^{-7} pF/√Hz. We are trying to demonstrate this level with the new GGG electronics)